J Biomol NMR (2010) 46:149–155
DOI 10.1007/s10858-009-9389-9

ARTICLE

High resolution NMR spectroscopy of nanocrystalline proteins at ultra-high magnetic field

Lindsay J. Sperling · Andrew J. Nieuwkoop · Andrew S. Lipton · Deborah A. Berthold · Chad M. Rienstra

Received: 24 August 2009 / Accepted: 27 October 2009 / Published online: 2 December 2009
© Springer Science+Business Media B.V. 2009

Abstract Magic-angle spinning (MAS) solid-state NMR (SSNMR) spectroscopy of uniformly-^{13}C,^{15}N labeled protein samples provides insight into atomic-resolution chemistry and structure. Data collection efficiency has advanced remarkably in the last decade; however, the study of larger proteins is still challenged by relatively low resolution in comparison to solution NMR. In this study, we present a systematic analysis of SSNMR protein spectra acquired at 11.7, 17.6 and 21.1 Tesla (^{1}H frequencies of 500, 750, and 900 MHz). For two protein systems—GB1, a 6 kDa nanocrystalline protein and DsbA, a 21 kDa nanocrystalline protein—line narrowing is demonstrated in all spectral regions with increasing field. Resolution enhancement is greatest in the aliphatic region, including methine, methylene and methyl sites. The resolution for GB1 increases markedly as a function of field, and for DsbA, resolution in the C–C region increases by 42%, according to the number of peaks that can be uniquely picked and integrated in the 900 MHz spectra when compared to the 500 MHz spectra. Additionally, chemical exchange is uniquely observed in the highest field spectra for at least two isoleucine Cδ1 sites in DsbA. These results further illustrate the benefits of high-field MAS SSNMR spectroscopy for protein structural studies.

Keywords Nanocrystalline proteins · Solid-state NMR spectroscopy · Spectral resolution · Ultra-high magnetic field

A. S. Lipton
Environmental Molecular Sciences Laboratory, Pacific Northwest National Laboratory, Richland, WA 99352, USA

L. J. Sperling · A. J. Nieuwkoop · D. A. Berthold · C. M. Rienstra (✉)
Department of Chemistry, University of Illinois at Urbana-Champaign, 600 South Mathews Avenue, Urbana, IL 61801, USA
e-mail: rienstra@scs.uiuc.edu

C. M. Rienstra
Department of Biochemistry, University of Illinois at Urbana-Champaign, 600 South Mathews Avenue, Urbana, IL 61801, USA

C. M. Rienstra
Center for Biophysics and Computational Biology, University of Illinois at Urbana-Champaign, 600 South Mathews Avenue, Urbana, IL 61801, USA

Introduction

Solid-state NMR (SSNMR) spectroscopy is a powerful tool for studying protein structure and function, uniquely able to address macroscopically disordered proteins. Insights from SSNMR include atomic-resolution structure, site-specific dynamics, metal center chemistry, and orientation of membrane proteins in bilayers (Smith and van Eck 1999; Baldus 2002; McDermott 2004; Opella and Marassi 2004). In recent years, methods have increasingly emphasized the use of uniformly-^{13}C,^{15}N-labeled samples to obtain site-specific information throughout an entire protein in each experiment, a capability for which high magnetic field has been demonstrated to be critical (McDermott et al. 2000; Pauli et al. 2001; Castellani et al. 2002; Bockmann et al. 2003; Igumenova et al. 2004a, b). In principle, this approach greatly enhances throughput and precision of analysis for large peptides and proteins; in practice, however, spectra may be insufficiently resolved to permit resonance assignments and subsequent analysis. To enhance resolution, investigators have made advances in isotopic labeling schemes (LeMaster and Kushlan 1996; Hong and

Jakes 1999), decoupling sequences (Bennett et al. 1995; Fung et al. 2000; Detken et al. 2002), and probe designs (Stringer et al. 2005; Doty et al. 2006; Dillmann et al. 2007).

Here we demonstrate systematically the benefits of using ultra-high magnetic fields for magic-angle spinning (MAS) spectra of proteins as nanocrystalline protein preparations. We demonstrate the experimental spectral resolution enhancement at ultra-high field with direct comparison of two proteins over a large range of resonance frequencies, including the highest magnetic field currently available for protein MAS studies (900 MHz). We observe a linear resolution benefit and find that chemical exchange is most prominent at ultra-high field.

Materials and methods

Sample preparation

DsbA has been successfully expressed in 100 mg quantities using an expression method described by Marley et al. (2001) *E. coli* containing DsbA expression plasmid were grown in unlabeled rich medium (LB) to generate large cell mass and then transferred to one-fourth volume of isotopically labeled minimal media prior to induction with IPTG. The cells were lysed by osmotic shock to release the periplasmic proteins. The procedure is intended to wash the cells with sucrose and then lyse the outer membrane with water, but we found that collecting the wash and the water supernatants increased the yield. DsbA was then purified by anion exchange chromatography, and ultimately oxidized with 5 mM glutathione and crystallized in a solution of 30% PEG 8000, 50 mM cacodylate pH 6.5, and 1.5% 2-methyl-2,4-pentanediol. The nanocrystalline solid was packed into limited speed 3.2-mm rotors. The preparation for GB1 has been previously reported (Franks et al. 2005).

SSNMR experiments

Spectra were acquired at B_0 fields of 11.7, 17.6, and 21.1 Tesla on a 500 MHz (^{1}H frequency) Varian Infinity Plus spectrometer, a 750 MHz (^{1}H frequency) Varian Unity Inova, and a 900 MHz (^{1}H frequency) Varian Unity Inova. MAS rates were 11.111 kHz at 500 MHz, 12.500 kHz at 750 MHz, and 13.333 kHz at 900 MHz. The 500 and 750 MHz data were acquired with Varian Balun^{TM} ^{1}H–^{13}C–^{15}N 3.2 mm probes, and the 900 MHz data were acquired with a Varian BioMAS^{TM} ^{1}H–^{13}C–^{15}N 3.2 mm probe in double resonance (^{1}H–^{13}C) mode (Stringer et al. 2005). The DsbA data were acquired on a 3.2 mm standard wall rotor with ~6 mg protein on the 750 MHz spectrometer, and on a 3.2 mm limited speed rotor with ~18 mg protein on the 500 and 900 MHz spectrometers. The GB1 data were acquired on three different 3.2 mm standard wall rotors with ~24 mg protein on the 750 and ~10 mg protein on the 500 MHz, and ~12 mg protein on the 900 MHz spectrometers. All pulse sequences utilized tangent ramped cross polarization (Hediger et al. 1994) with TPPM decoupling (Bennett et al. 1995) applied during the acquisition and evolution periods. The variable temperature gas was maintained at −10°C for DsbA with 100 scfh flow. The temperatures for GB1 varied at each field such that GB1 was maintained at 0°C for the 500 MHz experiments and −10°C for the 750 MHz experiments, and the 900 MHz experiments. Chemical shifts were referenced externally with adamantane (Morcombe and Zilm 2003). Data were processed with nmrPipe (Delaglio et al. 1995) with back linear prediction and polynomial baseline (frequency domain) correction applied to the direct dimension. Zero filling to 16,384 in the direct dimension and 8,192 in the indirect dimension was applied and Lorentzian-to-Gaussian apodization was employed for each dimension before Fourier transformation; further details with specifics for each spectrum are found in the respective figure captions.

Results and discussion

To minimize variations arising from technical details such as spectrometer electronics, probe design and sample preparations, we employed highly homologous instrument configurations and standard pulse sequences, applied to replica samples throughout this study. We prepared two proteins: (1) the 56 residue, 6 kDa immunoglobulin binding domain B1 of protein G, GB1 (Gronenborn et al. 1991; Franks et al. 2005) and (2) the 21 kDa soluble disulfide bond forming enzyme, DsbA. Each sample was packed in a limited speed 3.2-mm MAS rotor (Varian, Inc., Palo Alto, CA and Fort Collins, CO). Spectra were collected on three similar spectrometers and triple resonance ^{1}H–^{13}C–^{15}N probes (500 MHz Infinity Plus and 750 MHz Inova with Balun^{TM} ^{1}H–^{13}C–^{15}N probe at the University of Illinois at Urbana-Champaign; 900 MHz Inova with BioMAS^{TM} at the Pacific Northwest National Laboratories, Richland, WA), employing standard pulse sequences, including ^{1}H–^{13}C CP-MAS and two-dimensional (2D) ^{13}C–^{13}C with DARR mixing (Takegoshi et al. 2001; Morcombe et al. 2004) and carefully adjusted TPPM decoupling (Bennett et al. 1995). One can envision further improvements upon application of more recently developed pulse sequences.

GB1 was used initially to calibrate the instruments and assess the mixing time dependence of cross peak intensities (Fig. 1). We found the polarization transfer rates (at approximately the same MAS rates) to scale with the inverse

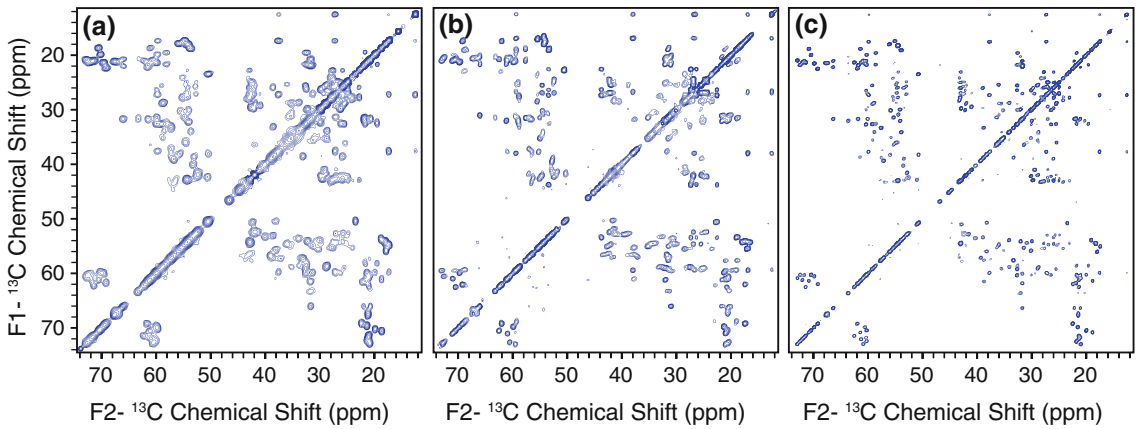

Fig. 1 Aliphatic region of 2D ^{13}C–^{13}C spectra of uniformly-^{13}C,^{15}N labeled GB1 acquired with DARR mixing on spectrometers with varying ^{1}H frequencies. **a** 500 MHz with 10 ms mixing (12 h); **b** 750 MHz with 25 ms mixing (5 h); **c** 900 MHz with 50 ms mixing (9.5 h). All spectra were processed identically, with 40 and 40 Hz Lorentzian-to-Gaussian line broadening in the direct and indirect dimensions, respectively

square of magnetic field. Thus subsequent 2D ^{13}C–^{13}C data sets were acquired with DARR mixing times of 50, 100, and 200 ms at 500, 750, and 900 MHz (^{1}H frequencies), respectively, to produce similar cross peak intensity patterns. Not only the rate but also the overall efficiency of mixing at higher field is decreased (based on the ratio of cross peak to diagonal intensity); therefore sensitivity in the 2D spectra cannot be accurately compared, and we focus subsequent discussion on the relative resolution of the spectra. Spectra were acquired with a minimum of 6 ms evolution in the indirect dimension (t_1) and 15 ms in the direct dimension (t_2), with appropriate apodization applied (net broadening was applied using a 1:2 Lorentzian-to-Gaussian function), prior to zero filling (8 and 16 k points, respectively), Fourier transformation, and baseline correction. Complete processing details and spectra for each protein are included in the figure captions.

Resolution enhancement can be easily observed in the GB1 spectra where at 500 MHz (^{1}H frequency) (Fig. 1a) there is some overlap of resonances, predominantly in the methyl region (Fig. 2a) close to the diagonal and in the Cα–Cβ region where peaks can not be baseline resolved from one another. At higher magnetic field, (Figs. 1b–c, 2b–c) the resolution is improved to the point that every peak in the 900 MHz (^{1}H frequency) spectra can be individually baseline resolved. The methyl region specifically shows amazing improvement since even the peaks that are close to the diagonal become resolved, not only from other cross peaks, but also from the diagonal itself.

This trend can also be seen in larger proteins, like DsbA, which shows the resolution enhancement with increasing magnetic field, just as GB1 does (Fig. 3). Although DsbA has a high degree of diversity of secondary structure elements (Martin et al. 1993; Guddat et al. 1998; Schirra et al.

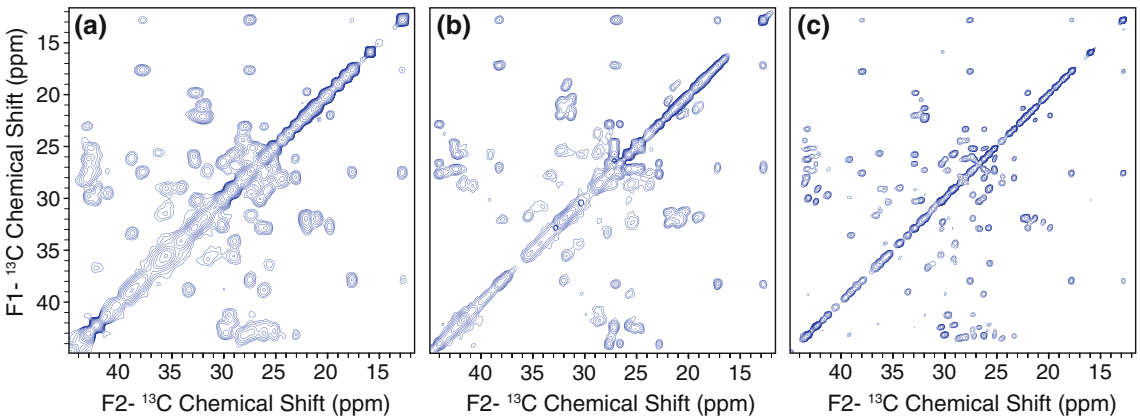

Fig. 2 Methyl region of 2D ^{13}C–^{13}C spectra of uniformly-^{13}C,^{15}N labeled GB1 acquired with DARR mixing on spectrometers with varying ^{1}H frequencies. **a** 500 MHz with 10 ms mixing (12 h); **b** 750 MHz with 25 ms mixing (5 h); **c** 900 MHz with 50 ms mixing (9.5 h). All spectra were processed identically, with 40 and 40 Hz Lorentzian-to-Gaussian line broadening in the direct and indirect dimensions, respectively

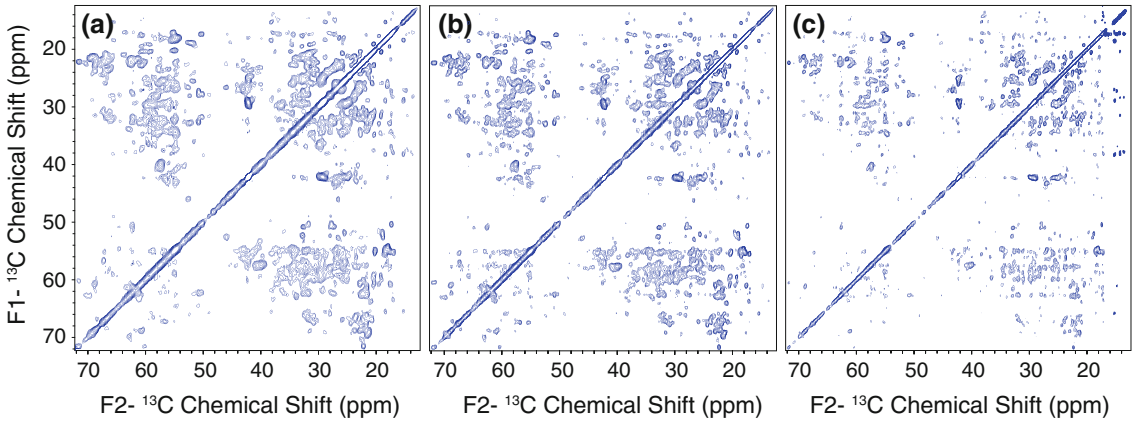

Fig. 3 Aliphatic region of 2D ^{13}C–^{13}C spectra of uniformly-^{13}C,^{15}N labeled wild type oxidized DsbA acquired with DARR mixing on spectrometers with varying ^{1}H frequencies. **a** 500 MHz with 50 ms mixing (9.6 h); **b** 750 MHz with 100 ms mixing (30 h); **c** 900 MHz with 200 ms mixing (27.5 h). All spectra were processed identically, with 15 and 35 Hz Lorentzian-to-Gaussian line broadening in the direct and indirect dimensions, respectively

1998) giving peaks within specific amino acids types greater chemical shift dispersion (Wishart and Sykes 1994; Cornilescu et al. 1999; Oldfield 2002), there are still many overlapped regions in the spectra.

The resolution enhancement is most prominently observed in the aliphatic Cα–Cβ region (Fig. 4) and the methyl region (Fig. 5) of the 2D ^{13}C–^{13}C DsbA spectra acquired at 500 MHz (Figs. 4a–5a), 750 MHz (Figs. 4b–5b), and 900 MHz (Figs. 4c–5c). Despite the presence of 189 residues in this protein, the majority of aliphatic correlations (55–65 ppm in F1, 25–40 ppm in F2) are uniquely resolved at 900 MHz (Fig. 4c). Although some chemical shift patterns (Ala, Thr, Val) are sufficiently resolved even at 500 MHz, the more congested methyl region (20–26 ppm in F2) illustrates a particularly significant improvement in resolution (Fig. 5). In the 900 MHz spectrum of DsbA, a total of 234 methyl peaks can be uniquely identified and integrated, compared with only 99 peaks in the 500 MHz spectrum.

To quantify the narrowing of all three proteins, comparisons of line widths for all resolved aliphatic resonances were made (limited by the number of sites resolved in the lower field spectra). Linewidths were determined in Sparky (Goddard and Kneller 2006) using Gaussian peak integration methods. Each protein was analyzed with the same protocol to compare line widths among data sets acquired at different magnetic fields. Peaks were chosen for analysis based on three prerequisite criteria: (1) signal-to-noise ratio greater than 10:1, (2) resolved in all three spectra, and (3) integrated with an experiment versus fit RMSD of 10% or less. The same set of peaks (resolution-limited by the lowest field data) was chosen for analysis among the three data sets acquired at 500, 750, and 900 MHz (^{1}H frequencies). Multiplet structure (arising from ^{13}C–^{13}C scalar

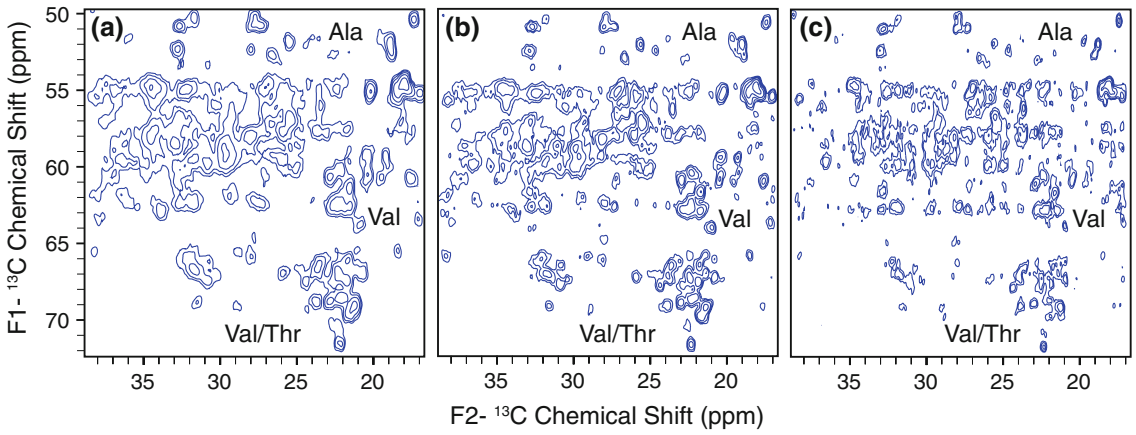

Fig. 4 Cα–Cβ region of 2D ^{13}C–^{13}C spectra of uniformly-^{13}C,^{15}N labeled wild type oxidized DsbA acquired with DARR mixing on spectrometers with varying ^{1}H frequencies. **a** 500 MHz with 50 ms mixing (9.6 h); **b** 750 MHz with 100 ms mixing (30 h); **c** 900 MHz with 200 ms mixing (27.5 h). All spectra were processed identically as noted in Fig. 3

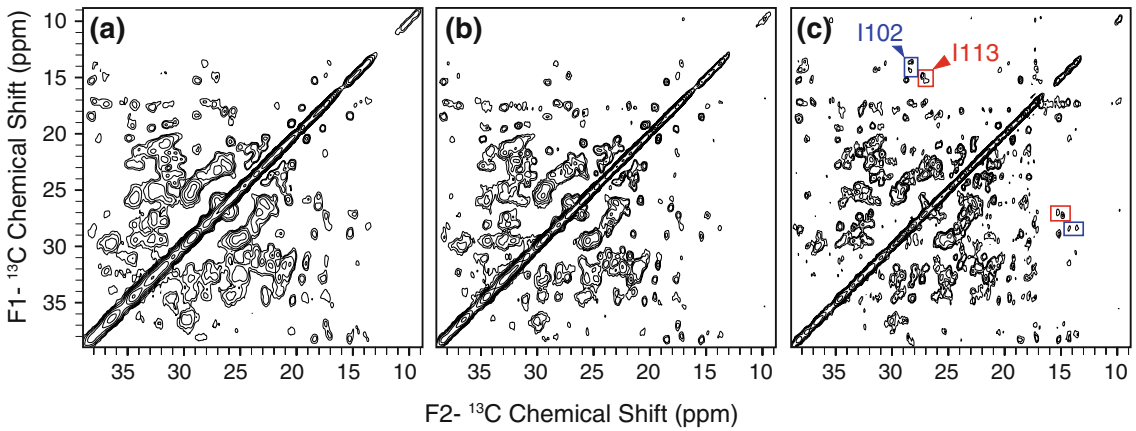

Fig. 5 Methyl region of 2D ^{13}C–^{13}C spectra of uniformly-^{13}C,^{15}N labeled wild type oxidized DsbA acquired with DARR mixing on spectrometers with varying ^{1}H frequencies. **a** 500 MHz with 50 ms mixing (9.6 h); **b** 750 MHz with 100 ms mixing (30 h); **c** 900 MHz with 200 ms mixing (27.5 h). All spectra were processed identically as noted in Fig. 3

couplings) was generally not observed due to the apodization functions employed; therefore the total line width includes contributions from homogeneous relaxation, multiplet structure and the line broadening added. These factors together result in overall line shapes that are well approximated by a Gaussian fitting function (as evidenced by the RMSD fit values of 10% or better in all cases, and typically better than 2%). The line widths are reported as the fitted line width minus the line broadening used. Plotting the line widths as a function of B_0 field (Fig. 6), we find a nearly linear improvement in resolution, arising from the approximately constant absolute line widths. This result indicates that the absolute homogeneous contributions to the linewidth (such as finite ^{1}H decoupling and residual ^{13}C–^{13}C dipolar couplings) are to first approximation invariant with magnetic field, and scalar couplings determine the absolute linewidth. In general all three spectral regions, including the methyl (CH_3; Fig. 6a), methine (CH; Fig. 6b), and methylene (CH_2; Fig. 6c) signals, show similar behavior for the two proteins (GB1, DsbA) with enhanced benefit from increased magnetic field.

In addition to the resolution enhancement, we observe signatures of chemical exchange solely at ultra-high magnetic fields. For example, in the methyl region of the 900 MHz DsbA spectrum, we observed two sets of chemical shifts for the side chain ^{13}C resonances (Cβ, Cδ1, Cγ1, and Cγ2) of I102 and I113 (Fig. 7c; Table 1). These intermediate-to-slow exchange events are more prominently

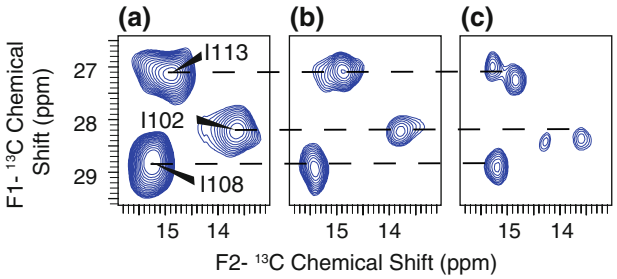

Fig. 7 Expansion of the Ile Cγ1–Cδ1 region of the ^{13}C–^{13}C 2D at **a** 500 MHz with 50 ms mixing (9.6 h); **b** 750 MHz with 100 ms mixing (30 h); **c** 900 MHz with 200 ms mixing (27.5 h). All spectra were processed identically

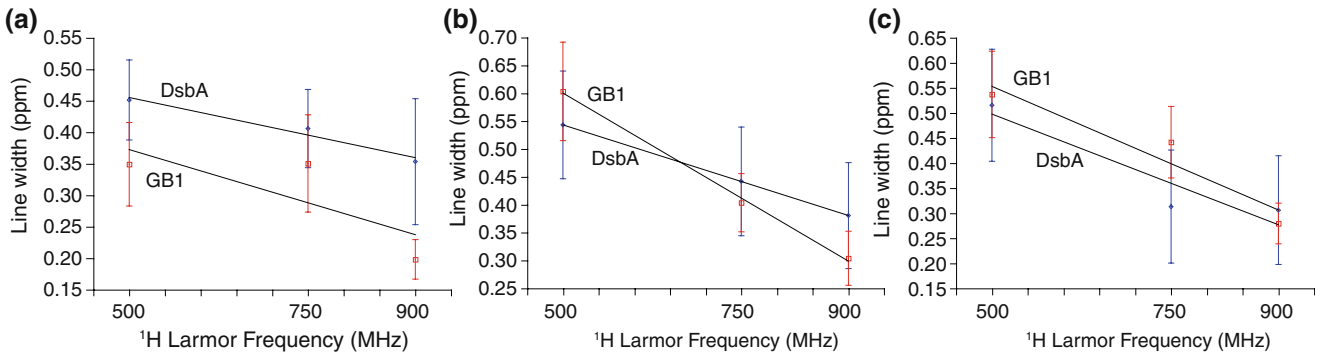

Fig. 6 Plot displaying the dependence of magnetic field strength on line widths for the **a** methyl, **b** methine and **c** methyene regions of ^{13}C–^{13}C 2Ds acquired on nanocrystalline DsbA and GB1. *Error bars* are drawn at 1σ

Table 1 Table of chemical shifts for Ile 102 and 113 observed in the 900 MHz (^{1}H frequency) data acquired on U–^{13}C,^{15}N labeled DsbA

Site	Chemical shift (ppm)	Error (ppm)	Difference (ppm)	Difference (Hz)
Ile102 Cα	61.13	0.05	0.00	0
Ile102 Cβ	37.03/37.19	0.10/0.04	0.16	36
Ile102 Cδ1	14.88/15.31	0.14/0.04	0.43	97
Ile102 Cγ1	27.23/26.98	0.03/0.05	0.25	57
Ile102 Cγ2	17.28/16.94	0.08/0.07	0.34	77
Ile113 Cα	63.49	0.01	0.00	0
Ile113 Cβ	37.92/38.21	0.15/0.10	0.29	66
Ile113 Cδ1	13.61/14.30	0.07/0.04	0.69	184
Ile113 Cγ1	28.30/28.40	0.03/0.02	0.10	23
Ile113 Cγ2	17.28/17.15	0.05/0.03	0.13	29

Where indicated, two numbers represent the unique resonance frequencies observed at high field. Spectra at 500 and 750 MHz are not sufficient to resolve the signals in this case

observed at high field, where the chemical shift difference significantly exceeds the exchange rate; conversely, slowing the exchange by decreasing temperature did not provide sufficiently well resolved spectra to identify the multiple conformations of Ile residues.

Conclusion

In conclusion, our experimental results illustrate that systematic and substantial resolution benefits are observed at ultra-high magnetic field. Here we evaluated these effects directly by comparison of practically identical samples at three magnetic fields, where most relevant hardware performance issues were highly similar. The improved resolution at ultra-high field promises to accelerate interpretation of MAS SSNMR data on large, macroscopically disordered proteins of broad interest, when used in combination with 3D experiments to establish ^{15}N correlations along the peptide backbone.

Acknowledgments The authors thank the National Institute of Heath for funding through NIGMS (GM073770), NIGMS/Roadmap Initiative (GM075937) and Molecular Biophysics Training Grant (to LJS and AJN), David Hoyt, Jesse Sears, and Paul Ellis at the Environmental Molecular Science Laboratory (a national scientific user facility sponsored by the Department of Energy Office of Biological and Environmental Research) located at Pacific Northwest National Laboratory and operated for DOE by Batelle for their assistance in acquiring the 900 MHz data, Dr. Donghua Zhou for pulse sequence code, Dr. Trent Franks and Benjamin Fisher of the VOICE NMR Facility for technical assistance.

References

Baldus M (2002) Correlation experiments for assignment and structure elucidation of immobilized polypeptides under magic angle spinning. Prog Nucl Magn Reson Spectrosc 41:1–47

Bennett AE, Rienstra CM, Auger M, Lakshmi KV, Griffin RG (1995) Heteronuclear decoupling in rotating solids. J Chem Phys 103:6951–6958

Bockmann A, Lange A, Galinier A, Luca S, Giraud N, Juy M, Heise H, Montserret R, Penin F, Baldus M (2003) Solid state NMR sequential resonance assignments and conformational analysis of the 2 × 10.4 kDa dimeric form of the *Bacillus subtilis* protein Crh. J Biomol NMR 27:323–339

Castellani F, van Rossum B, Diehl A, Schubert M, Rehbein K, Oschkinat H (2002) Structure of a protein determined by solid-state magic-angle spinning NMR spectroscopy. Nature 420:98–102

Cornilescu G, Delaglio F, Bax A (1999) Protein backbone angle restraints from searching a database for chemical shift and sequence homology. J Biomol NMR 13:289–302

Delaglio F, Grzesiek S, Vuister GW, Zhu G, Pfeifer J, Bax A (1995) NMRPipe—a multidimensional spectral processing system based on Unix Pipes. J Biomol NMR 6:277–293

Detken A, Hardy EH, Ernst M, Meier BH (2002) Simple and efficient decoupling in magic-angle spinning solid-state NMR: the XiX scheme. Chem Phys Lett 356:298–304

Dillmann B, Elbayed K, Zeiger H, Weingertner MC, Plotto M, Engelke F (2007) A novel low-E field coil to minimize heating of biological samples in solid-state multinuclear NMR experiments. J Magn Reson 187:10–18

Doty FD, Kulkarni J, Turner C, Entzminger G, Bielecki A (2006) Using a cross-coil to reduce RF heating by an order of magnitude in triple-resonance multinuclear MAS at high fields. J Magn Reson 182:239–253

Franks WT, Zhou DH, Wylie BJ, Money BG, Graesser DT, Frericks HL, Sahota G, Rienstra CM (2005) Magic-angle spinning solid-state NMR spectroscopy of the beta1 immunoglobulin binding domain of protein G (GB1): ^{15}N and ^{13}C chemical shift assignments and conformational analysis. J Am Chem Soc 127:12291–12305

Fung BM, Khitrin AK, Ermolaev K (2000) An improved broadband decoupling sequence for liquid crystals and solids. J Magn Reson 142:97–101

Goddard TD, Kneller DG (2006) Sparky 3. University of California, San Francisco

Gronenborn AM, Filpula DR, Essig NZ, Achari A, Whitlow M, Wingfield PT, Clore GM (1991) A novel, highly stable fold of the immunoglobulin binding domain of streptococcal protein-G. Science 253:657–661

Guddat LW, Bardwell JCA, Martin JL (1998) Crystal structures of reduced and oxidized DsbA: investigation of domain motion and thiolate stabilization. Structure 6:757–767

Hediger S, Meier BH, Kurur ND, Bodenhausen G, Ernst RR (1994) NMR cross-polarization by adiabatic passage through the Hartmann-Hahn condition (APHH). Chem Phys Lett 223:283–288

Hong M, Jakes K (1999) Selective and extensive ^{13}C labeling of a membrane protein for solid-state NMR investigations. J Biomol NMR 14:71–74

Igumenova TI, McDermott AE, Zilm KW, Martin RW, Paulson EK, Wand AJ (2004a) Assignments of carbon NMR resonances for microcrystalline ubiquitin. J Am Chem Soc 126:6720–6727

Igumenova TI, Wand AJ, McDermott AE (2004b) Assignment of the backbone resonances for microcrystalline ubiquitin. J Am Chem Soc 126:5323–5331

LeMaster DM, Kushlan DM (1996) Dynamical mapping of *E. coli* thioredoxin via ^{13}C NMR relaxation analysis. J Am Chem Soc 118:9255–9264

Marley J, Lu M, Bracken C (2001) A method for efficient isotopic labeling of recombinant proteins. J Biomol NMR 20:71–75

Martin JL, Bardwell JCA, Kuriyan J (1993) Crystal structure of the DsbA protein required for disulphide bond formation in vivo. Nature 365:464–468

McDermott AE (2004) Structural and dynamic studies of proteins by solid-state NMR spectroscopy: rapid movement forward. Curr Opin Struct Biol 14:554–561

McDermott A, Polenova T, Bockmann A, Zilm KW, Paulson EK, Martin RW, Montelione GT (2000) Partial NMR assignments for uniformly (^{13}C, ^{15}N)-enriched BPTI in the solid state. J Biomol NMR 16:209–219

Morcombe CR, Zilm KW (2003) Chemical shift referencing in MAS solid state NMR. J Magn Reson 162:479–486

Morcombe CR, Gaponenko V, Byrd RA, Zilm KW (2004) Diluting abundant spins by isotope edited radio frequency field assisted diffusion. J Am Chem Soc 126:7196–7197

Oldfield E (2002) Chemical shifts in amino acids, peptides, and proteins: from quantum chemistry to drug design. Ann Rev Phys Chem 53:349–378

Opella SJ, Marassi FM (2004) Structure determination of membrane proteins by NMR spectroscopy. Chem Rev 104:3587–3606

Pauli J, Baldus M, van Rossum B, de Groot H, Oschkinat H (2001) Backbone and side-chain ^{13}C and ^{15}N resonance assignments of the alpha-spectrin SH3 domain by magic angle spinning solid state NMR at 17.6 Tesla. ChemBioChem 2:101–110

Schirra HJ, Renner C, Czisch M, Huber-Wunderlich M, Holak TA, Glockshuber R (1998) Structure of reduced DsbA from *Escherichia coli* in solution. Biochemistry 37:6263–6276

Smith ME, van Eck ERH (1999) Recent advances in experimental solid state NMR methodology for half-integer spin quadrupolar nuclei. Prog Nucl Magn Reson Spectrosc 34:159–201

Stringer JA, Bronnimann CE, Mullen CG, Zhou DH, Stellfox SA, Li Y, Williams EH, Rienstra CM (2005) Reduction of RF-induced sample heating with a scroll coil resonator structure for solid-state NMR probes. J Magn Reson 173:40–48

Takegoshi K, Nakamura S, Terao T (2001) ^{13}C–^{1}H dipolar-assisted rotational resonance in magic-angle spinning NMR. Chem Phys Lett 344:631–637

Wishart DS, Sykes BD (1994) The ^{13}C chemical-shift index: a simple method for the identification of protein secondary structure using ^{13}C chemical-shift data. J Biomol NMR 4:171–180